EES Solar

REVIEW

View Article Online
View Journal | View Issue

Cite this: *EES Sol.*, 2025, **1**, 681

Photocatalytic ammonia decomposition for hydrogen generation: insights from gas-phase and liquid-phase pathways

Qian Lei,†[a] Huazhang Feng,†[a] Yuankai Li[a] and Jung Kyu Kim *[ab]

Ammonia as a carbon-free nitrogenous compound has emerged as a promising hydrogen carrier for next-generation sustainable energy systems due to its high hydrogen density, low production cost, and ease of storage and transport. Nevertheless, current industrial activities have led to excessive ammonia emissions, including both gaseous and aqueous states, which results in serious environmental damage. Ammonia degradation for hydrogen generation can not only address the environmental issues, but also offer a solution to the energy crisis. In recent years, photocatalytic conversion of ammonia into hydrogen has emerged as a promising strategy due to its significant potential in sustainability and economic practicality. This review presents a comprehensive overview of recent progress in the development of advanced photocatalysts for ammonia splitting in gaseous and aqueous phases to produce hydrogen. Finally, key challenges and perspectives in future research based on photocatalytic NH_3 conversion are discussed. This review provides guidance for the rational design of next-generation photocatalytic systems.

Received 30th April 2025
Accepted 2nd August 2025

DOI: 10.1039/d5el00067j

rsc.li/EESSolar

Broader context

Ammonia has attracted significant interest as a promising hydrogen storage medium to support the development of green hydrogen economy owing to its ease of storage and transport. However, excessive ammonia emissions from industrial activities into both atmospheric and aquatic environments have raised serious concerns, including toxicity, eutrophication, and secondary pollution. In recent years, photocatalytic ammonia decomposition to generate hydrogen has shown significant potential for highly efficient ammonia conversion due to its low cost, environmental friendliness, and safety. This review first elucidates the reaction mechanisms involved in photocatalytic ammonia degradation for hydrogen production. Then, it summarizes the reported photocatalysts and their performance in both gas-phase and liquid-phase systems. Finally, the review outlines the key challenges and future research directions to inform the rational development of photocatalysis-driven systems toward ammonia-based hydrogen economies. We believe this review will provide guidance for the rational design of next-generation photocatalytic systems.

1. Introduction

The excessive exploitation of traditional energy sources including coal, oil, and natural gas has raised serious concerns about resource depletion and environmental deterioration. In order to solve these issues, the development of more efficient and eco-friendly technologies for energy storage and conversion has attracted great attention,[1,2] particularly those based on renewable energy sources such as tidal energy, solar energy, and wind power.[3,4] Among the various alternatives, hydrogen (H_2) is considered as a promising and efficient source due to its high energy density (142 MJ kg^{-1}) and zero carbon emissions.[5–7] This makes it a feasible alternative to traditional fossil fuels. However, the widespread adoption of hydrogen energy is hindered by its storage and transportation.[8] Given these challenges, ammonia (NH_3) emerges as a carbon-free carrier of H_2, offering the highest gravimetric (17.8%) and volumetric hydrogen density (121 kg H_2 per m^3 at 10 bar) among other H_2 carriers and can be liquefied at room temperature under mild conditions (8.6 bar).[9,10] Compared to water splitting, ammonia decomposition requires significantly less energy, demonstrating its higher energy efficiency, as shown in eqn (1)–(3). These properties make ammonia an ideal medium for hydrogen storage and transportation, facilitating the transition to a hydrogen-based economy.[11–13]

$$H_2O(I) = \frac{1}{2}O_2(g) + H_2(g) \quad \Delta G^\circ = 237.1\ \text{kJ mol}^{-1} \qquad (1)$$

$$NH_3(g) = \frac{1}{2}N_2(g) + \frac{3}{2}H_2(g) \quad \Delta G^\circ = 16.4\ \text{kJ mol}^{-1} \qquad (2)$$

$$NH_3(aq) = \frac{1}{2}N_2(g) + \frac{3}{2}H_2(g) \quad \Delta G^\circ = 27\ \text{kJ mol}^{-1} \qquad (3)$$

[a]*School of Chemical Engineering, Sungkyunkwan University (SKKU), Suwon 16419, Republic of Korea. E-mail: legkim@skku.edu*

[b]*SKKU Advanced Institute of Nanotechnology (SAINT), Sungkyunkwan University (SKKU), Suwon 16419, Republic of Korea*

† These authors contributed equally to this work.

In addition to its role as a hydrogen carrier, ammonia is widely used in several industrial sectors, most notably in fertilizer production, refrigeration systems and chemical manufacturing processes.[14–16] However, the widespread use of ammonia raises significant environmental and public health concerns. As a toxic and pungent atmospheric pollutant, ammonia gas is emitted in substantial quantities from both anthropogenic and natural sources.[17,18] Once released into the atmosphere, NH_3 readily reacts with acidic gases like sulfur dioxide (SO_2) and nitrogen oxides (NO_x) to form secondary inorganic aerosols, which are key precursors of atmospheric haze and fine particulate matter (PM2.5).[19,20] Moreover, ammonia's corrosive and irritating properties pose serious threats to human health and safety.[21] On the other hand, the wide presence of aqueous ammonia in industrial wastewater and agricultural runoff poses a significant threat to aquatic ecosystems and human health. Even at low concentrations, NH_3 exhibits high toxicity toward aquatic organisms, disrupting nitrogen cycling and promoting eutrophication.[22] In addition, NH_3 contamination of drinking water can cause neurological and organ damage.[23,24] According to the European Environment Agency, ammonia emissions currently exceed 3000 tonnes, with more than 80% attributed to fertilizer usage and animal waste management.[25] Considering these pressing environmental and health challenges, the development of efficient ammonia removal or conversion technologies is necessary to eliminate its harmful impacts. Therefore, the catalytic decomposition of NH_3 into H_2 has emerged as a compelling solution that transforms the pollutant into a valuable clean energy carrier (Scheme 1).

The decomposition of NH_3 into H_2 is a critical step to realize a carbon-neutral and hydrogen economy. To this end, various NH_3-to-H_2 conversion technologies have been explored. Conventional approaches rely on thermocatalytic processes.[26] In this approach, NH_3 is introduced into a fixed-bed reactor

Qian Lei

Qian Lei is currently a PhD student under the supervision of Prof. Jung Kyu Kim in the School of Chemical Engineering, Sungkyunkwan University (SKKU), Republic of Korea. She received her master's degree from the School of Electronic Information and Optical Engineering, Taiyuan University of Technology, China in 2023. Her research mainly focuses on photoelectrochemical cells for high-efficiency energy conversion.

Yuankai Li

Yuankai Li is currently a postdoc researcher at the School of Chemical Engineering in Sungkyunkwan University (SKKU) since 2025. He received his PhD under the supervision of Prof. Jung Kyu Kim in the School of Chemical Engineering, Sungkyunkwan University in 2025. He received his master's degree from the School of Instrument and Electronics, North University of China, China in 2020. His research focuses on metal oxide nanostructures for photo/electrochemical cells.

Huazhang Feng

Huazhang Feng is currently a PhD student under the supervision of Prof. Jung Kyu Kim in the School of Chemical Engineering, Sungkyunkwan University (SKKU), Republic of Korea. He received his master's degree in materials and chemical engineering from Shenzhen University, China in 2023. His research mainly focuses on photocatalytic processes for clean energy conversion.

Jung Kyu Kim

Jung Kyu Kim is currently a tenure-track associate professor at the School of Chemical Engineering, and SKKU Advanced Institute of Nano Technology in Sungkyunkwan University. He received his bachelor's, MS, and PhD degrees in Chemical Engineering, and Nano-science & Technology from Sungkyunkwan University in 2010, 2012 and 2015, respectively. Prior to joining Sungkyunkwan University in 2018, he did his postdoctoral work in the Department of Mechanical Engineering at Stanford University (2015–2018). His research group focuses on diverse nanomaterials and devices for energy conversions and storage with environmental friendliness and high sustainability including solar-to-electric, solar-to-electrochemical, and electric-to-chemical energy conversions.

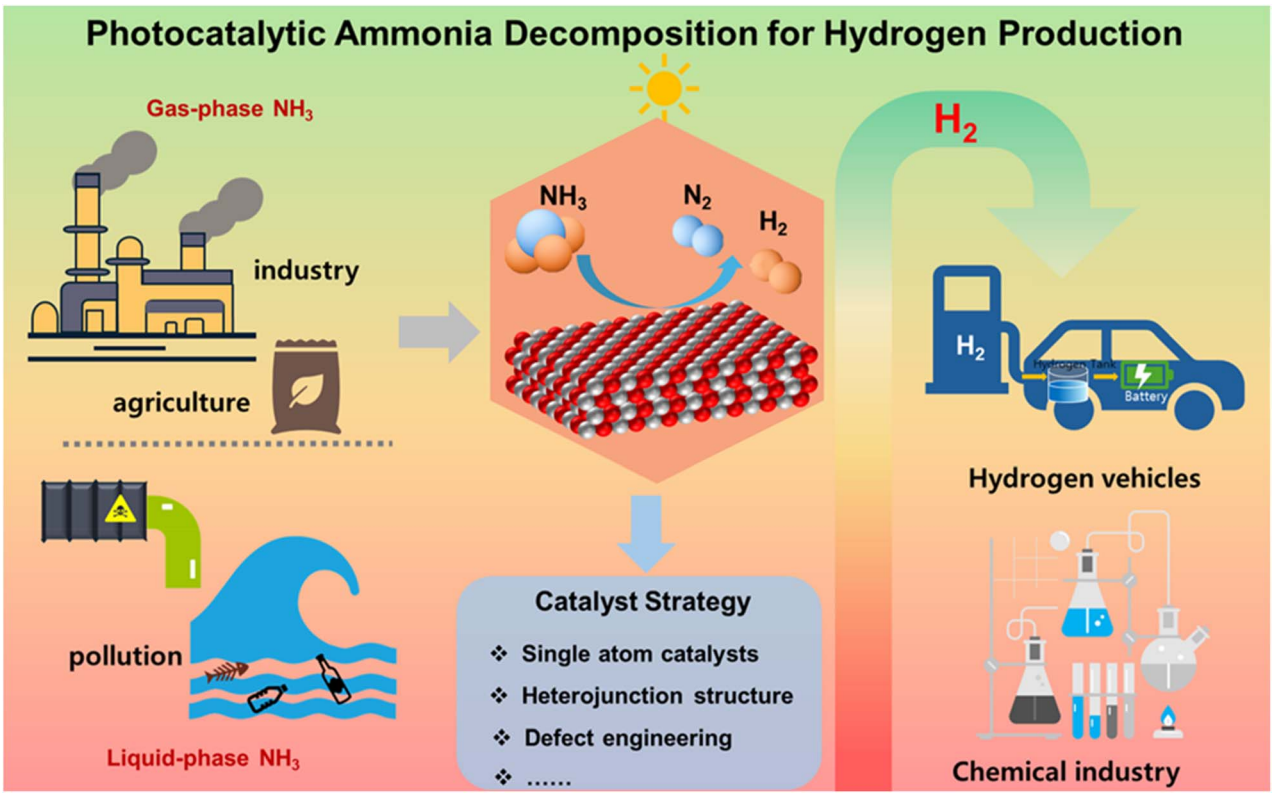

Scheme 1 Photocatalytic decomposition of gaseous and liquid ammonia for hydrogen production: addressing environmental and energy challenges.

containing a solid catalyst and maintained at elevated temperatures (typically 400–600 °C), where it undergoes endothermic decomposition into N_2 and H_2.[27,28] The product gases are then separated and purified to produce high-purity H_2 for downstream applications.[29] Unfortunately, this thermocatalytic process requires a large amount of energy input, which increases the operating costs.[30] In addition, thermocatalytic systems typically rely on expensive noble metal catalysts (*e.g.*, Pt, Ru, and Ir), which are easily deactivated due to sintering and poisoning under prolonged operation.[31] These drawbacks have stimulated growing interest in developing alternative, energy-efficient strategies for ammonia decomposition. Among the emerging alternatives, photocatalytic ammonia decomposition has attracted increasing attention due to its potential for low energy input and environmental friendliness.[32] Unlike thermocatalytic systems that rely on high-temperature furnaces and costly noble metals,[33] photocatalytic approaches utilize semiconductors to harvest solar energy and drive redox reactions at room temperature, which can not only reduce operational costs but also minimize the formation of harmful byproducts such as NO_x.[34] Common photocatalysts for ammonia decomposition include transition metal oxides (*e.g.*, TiO_2 and WO_3) for their stability and bandgap tunability, noble metals (*e.g.*, Ru and Pt), which act as efficient cocatalysts, and emerging materials like g-C_3N_4 and MOFs for their tailored photoactivity and surface properties.[35] Therefore, photocatalytic NH_3 conversion represents a promising and sustainable pathway for clean hydrogen production and environmental remediation.

In this review, we provide a comprehensive overview of recent advances in photocatalytic ammonia (NH_3) decomposition for hydrogen production, across both gaseous and aqueous phases. Considering the dual environmental-health threats posed by gaseous and aqueous NH_3 pollution, as well as the great potential of photocatalysis as a sustainable and efficient treatment strategy, a holistic assessment of current technologies and hydrogen production pathways is very necessary. This review first elucidates the reaction mechanisms involved in photocatalytic ammonia degradation for hydrogen production. Then, it summarizes the reported photocatalysts and their performance in both gas-phase and liquid-phase systems. Finally, the review outlines the key challenges and future research directions to inform the rational development of photocatalysis-driven systems toward ammonia-based hydrogen economy.

2. Fundamental principles of photocatalytic ammonia decomposition

Photocatalysis, driven by intermittent solar irradiation, is an environmentally friendly process that is not constrained by geographical limitations. It has demonstrated significant

potential across diverse fields including energy conversion, environmental remediation, artificial photosynthesis, and healthcare applications.[36–38] A typical photocatalytic reaction proceeds through three key steps: (1) light absorption and generation of photogenerated carriers; (2) separation and transfer of photogenerated holes and electrons to the photocatalyst surface; (3) surface reactions between the charge carriers and substrate molecules.[39,40] The overall efficiency is jointly determined by the performance of these three steps. However, the inherent band structure of the photocatalysts often limits their ability to harvest solar energy effectively.[41] Moreover, intrinsic bulk defects within the material can accelerate the recombination of photogenerated charge carriers, thereby reducing the efficiency of charge separation.[42] Additionally, insufficient surface reaction sites can hinder the timely consumption of electrons and holes, leading to undesired recombination. To overcome the limitations of conventional photocatalysts, several strategies have been extensively explored, including heterojunction construction, defect engineering, and cocatalyst loading. Heterojunctions improve charge separation, enhance light absorption, and optimize band alignment, thereby boosting multiple aspects of photocatalytic efficiency. Defect engineering introduces active sites that modulate the electronic structure and facilitate the adsorption and activation of reactants. Cocatalyst loading accelerates redox kinetics, promotes charge separation, and improves catalyst stability by suppressing carrier recombination and mitigating photocorrosion.[43–47]

Beyond general photocatalytic processes, ammonia decomposition introduces additional challenges owing to the dual-phase nature of ammonia (liquid and gas at room temperature). Thus, besides catalyst design, the construction of a suitable reaction environment becomes equally critical. Compared to the more widely studied photocatalytic water splitting for hydrogen production, ammonia decomposition is more complex. To avoid the formation of undesired oxidation byproducts (such as NO_x/N_2O/HONO in the gas phase and NO_3^-/NO_2^- in the aqueous phase, which may appear as intermediate or final products), it is crucial to conduct photocatalytic ammonia decomposition under oxygen-free conditions to achieve the production of hydrogen and harmless nitrogen. Various reaction pathways have been proposed for photocatalytic ammonia decomposition. Initially, ammonia molecules are adsorbed onto the photocatalyst surface and interact with photogenerated holes to form ammonia radicals, a step widely regarded as rate-determining, and then two main pathways are possible (Fig. 1a).[48] In Route 1, ammonia radicals undergo successive dehydrogenation *via* hole interactions to form nitrogen radicals, which subsequently couple to yield N_2. In Route 2, two ammonia radicals directly couple, followed by dehydrogenation steps to produce N_2 and H_2. Density functional theory (DFT) calculations indicate that Route 2 has lower activation energy, suggesting that it is thermodynamically more favourable. Similar conclusions have been reported in other related studies (Fig. 1b).[49] Furthermore, a detailed mechanism has been proposed for the decomposition of hydrazine (N_2H_4), an intermediate generated during radical coupling in Route 2. Upon light irradiation, N_2H_4 can dehydrogenate to form diazene (N_2H_2), which either spontaneously decomposes into N_2 and H_2 or undergoes a disproportionation reaction to yield N_2 and regenerate N_2H_4, allowing the catalytic cycle to continue.

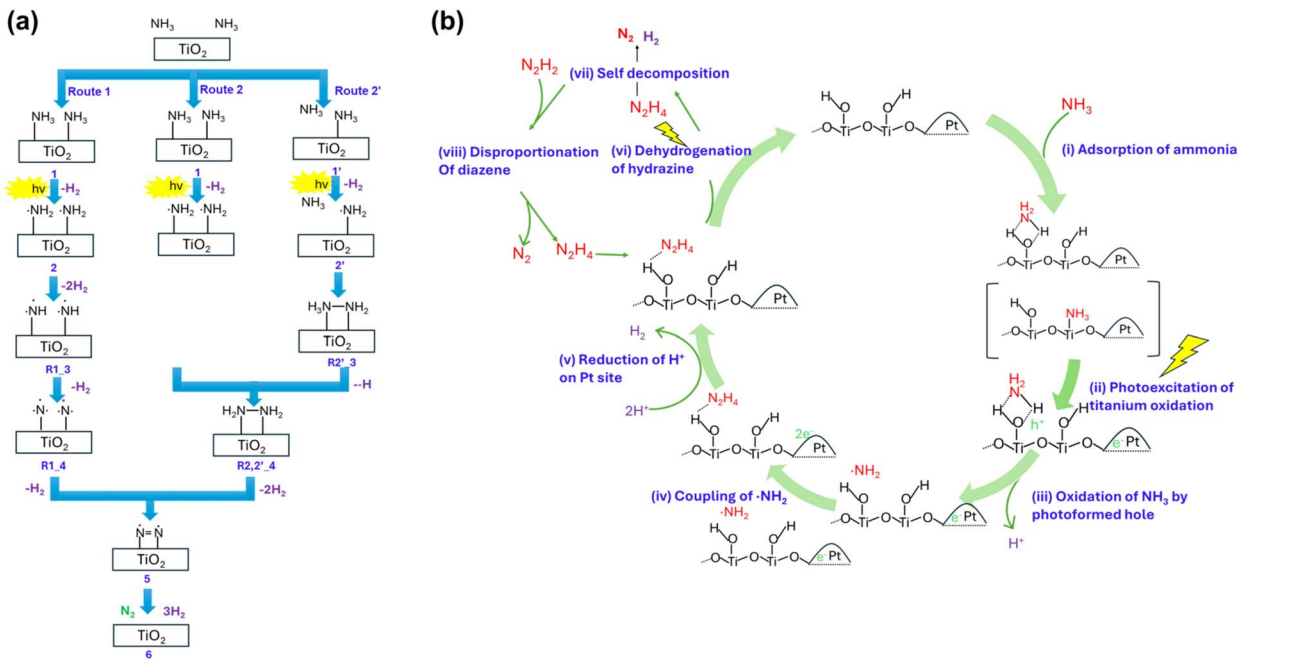

Fig. 1 (a) Suggested reaction mechanism for NH_3 decomposition to N_2 and H_2 over the TiO_2 photocatalyst.[48] Copyright 2017, Elsevier. (b) Proposed dominant reaction path of the photocatalytic ammonia decomposition on platinum loaded titanium oxide in the presence of water.[49] Copyright 2012, American Chemical Society.

In liquid systems, the ammonia degradation process typically proceeds through the N_2H_y dehydrogenation mechanism, wherein NH_x intermediates couple to form N_2H_y species, which subsequently undergo stepwise dehydrogenation to yield molecular nitrogen. Conversely, in gas-phase environments, the reaction is more commonly governed by the N–N recombination mechanism, involving the direct coupling of nitrogen-containing species to form N_2.[50]

3. Photocatalytic ammonia decomposition to hydrogen in the gaseous phase

Gaseous ammonia is a byproduct of agriculture, industry and waste management. Excessive emissions will cause air pollution and damage to the nitrogen cycle of ecosystems. At the same time, ammonia is also a valuable source of hydrogen. Therefore, it is urgent to develop efficient photocatalytic strategies that can both control pollution and recover hydrogen. Rational design and selection of photocatalysts are key to achieving this dual function. An effective catalyst should have sufficient interactions to activate the reactants while allowing the products to desorb in a timely manner, thereby alleviating the kinetic barriers associated with the adsorption and desorption steps.[51,52] Due to the unique ability of metal nanoparticles to collect and utilize nonequilibrium carriers generated by photoexcitation, recent research progress has highlighted the important prospects of metal nanoparticles as active components for hot-carrier-mediated photocatalysis.[53] Metal NPs exhibit localized surface plasmon resonances (LSPRs), which play an important role in promoting the generation of hot-carriers.[54] In plasmon-enhanced catalysis, the presence of hot carriers promotes a synergistic interaction with thermal energy to overcome the kinetic barriers. Inspired by this concept, Zhou *et al.* explored its applicability in ammonia decomposition by

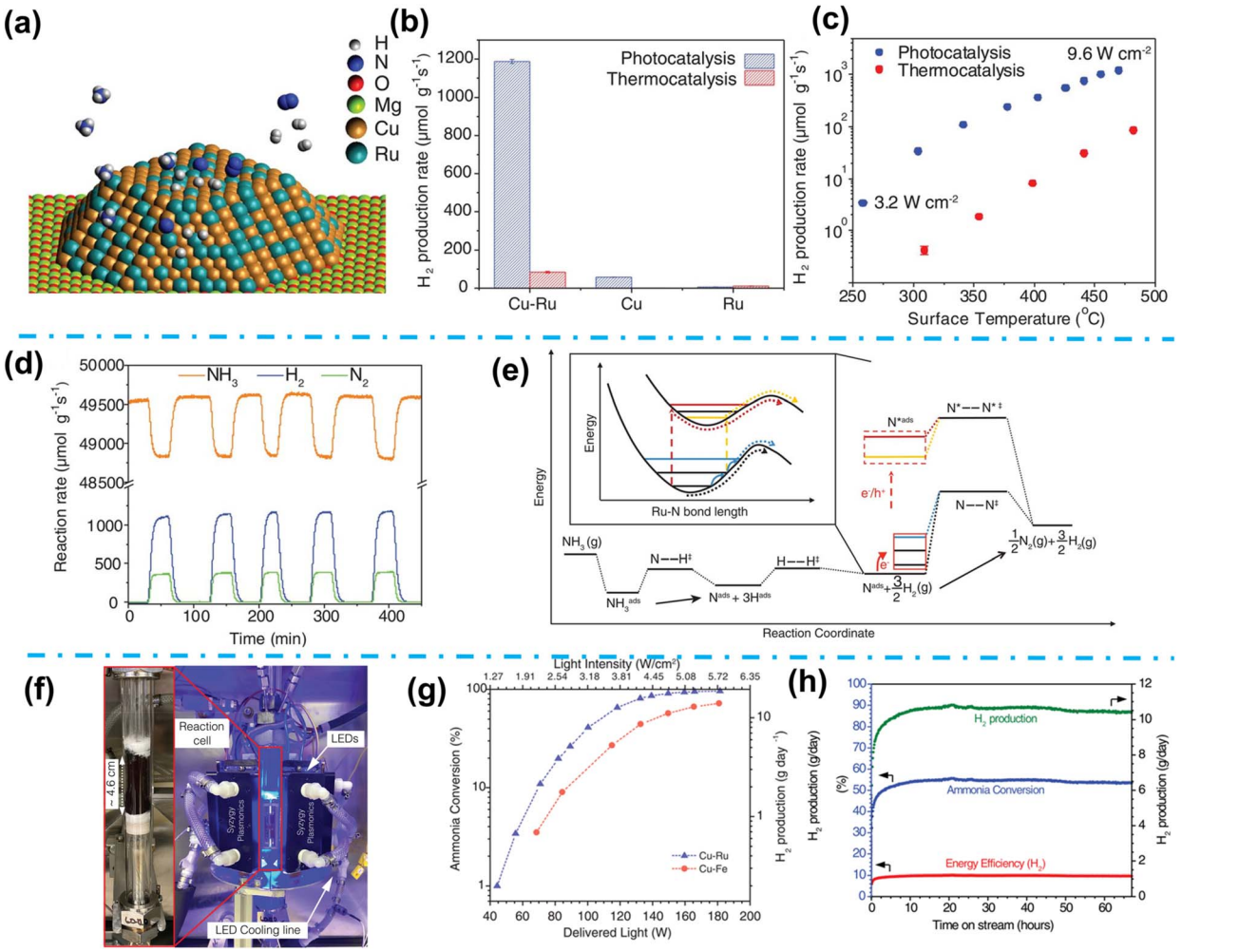

Fig. 2 (a) Schematic of the structure of Cu-Ru-AR. (b) H_2 formation rate of photocatalysis. (c) Comparison of photocatalytic and thermostatic rates on Cu-Ru-AR. (d) Photocatalytic rates on Cu-Ru-AR under white-light illumination without external heating. (e) Schematic energetics of elementary reaction steps for NH_3 decomposition.[55] Copyright 2018, American Association for the Advancement of Science. (f) Photograph of the reaction cell (left) and the photocatalytic platform (right) for ammonia decomposition. (g) Ammonia conversion and corresponding H_2 production rates and (h) long-term photocatalytic ammonia decomposition.[56] Copyright 2022, American Association for the Advancement of Science.

employing a plasmonic antenna–reactor (AR) architecture to facilitate hot-carrier-mediated activation pathways.[55] In their research, a Cu-Ru antenna–reactor (Cu-Ru-AR) nanostructure was developed, in which Cu nanoparticles acted as plasmonic antennas for efficient light harvesting, while adjacent Ru sites functioned as catalytic centers to drive ammonia decomposition (Fig. 2a). This antenna–reactor design significantly enhanced the catalytic activity, with NH_3 decomposition rates being 20 and 177 times higher than those of pure Cu and Ru nanoparticles, respectively (Fig. 2b). Under light irradiation without external heating, the system achieved a decomposition rate of 1200 μmol H_2 per g per s (Fig. 2c). After stopping the light, the activity rapidly dropped to the thermal baseline, confirming the critical role of photogenerated hot carriers (Fig. 2d). As shown in the energy profile of the reaction pathway (Fig. 2e), the hot carriers contribute to lowering the energy barrier of the rate-determining step by promoting the activation of adsorbed nitrogen intermediates (N_ads). Additionally, photogenerated electrons and holes transferred to the Ru–N surface facilitating N_2 desorption, thereby enhancing the overall kinetics of ammonia decomposition.

While significant progress has been made, the scarcity and high cost of Ru pose significant limitations to the feasibility and scalability of this catalytic system. To address this challenge, Halas *et al.* explored the use of earth-abundant transition metals, such as Fe, as substitutes for Ru to improve economic viability and scalability in plasmon-assisted ammonia decomposition.[56] Utilizing a scalable, LED-driven, high-throughput photoreactor developed by Syzygy Plasmonics, they employed Cu-Fe and Cu-Ru antenna–reactor nanostructures (Fig. 2f). Under pulsed light irradiation, hot carriers were generated, which activate the metal-adsorbate interactions, lower the energy barriers of the key reaction steps, and promote the efficient desorption of the products. As a result, the Cu-Fe-AR system achieved a remarkable 72% NH_3 conversion and produced 14 g of H_2 per day, outperforming the Ru-based counterpart (Fig. 2g). Furthermore, the system demonstrated excellent long-term stability (Fig. 2h).

By shrinking metal nanoclusters to the atomic scale, individual metal atoms can be dispersed on a suitable support to form isolated and uniform active sites. This structural configuration significantly improves the intrinsic catalytic activity and makes the metal atom utilization rate close to 100%. Catalysts with atomically dispersed metals coordinated with supports are known as single-atom catalysts (SACs), representing a new frontier in heterogeneous catalysis. Given the unique properties exhibited by SACs, they are regarded as a potentially viable candidate for photocatalytic ammonia degradation.[57] Lin *et al.* were the first to synthesize a microporous carbon nitride-supported nickel single-atom transition metal (Ni-MCN) catalyst for solar-driven photocatalytic gaseous NH_3 splitting,[58] as illustrated in Fig. 3a. In their work, the Ni-1.4-MCN catalyst successfully replicated the ordered architecture of the silica colloidal crystal template, resulting in a well-defined microporous structure (Fig. 3b). The photocatalytic ammonia splitting activity of a series of TMs-MCN SACs was evaluated using

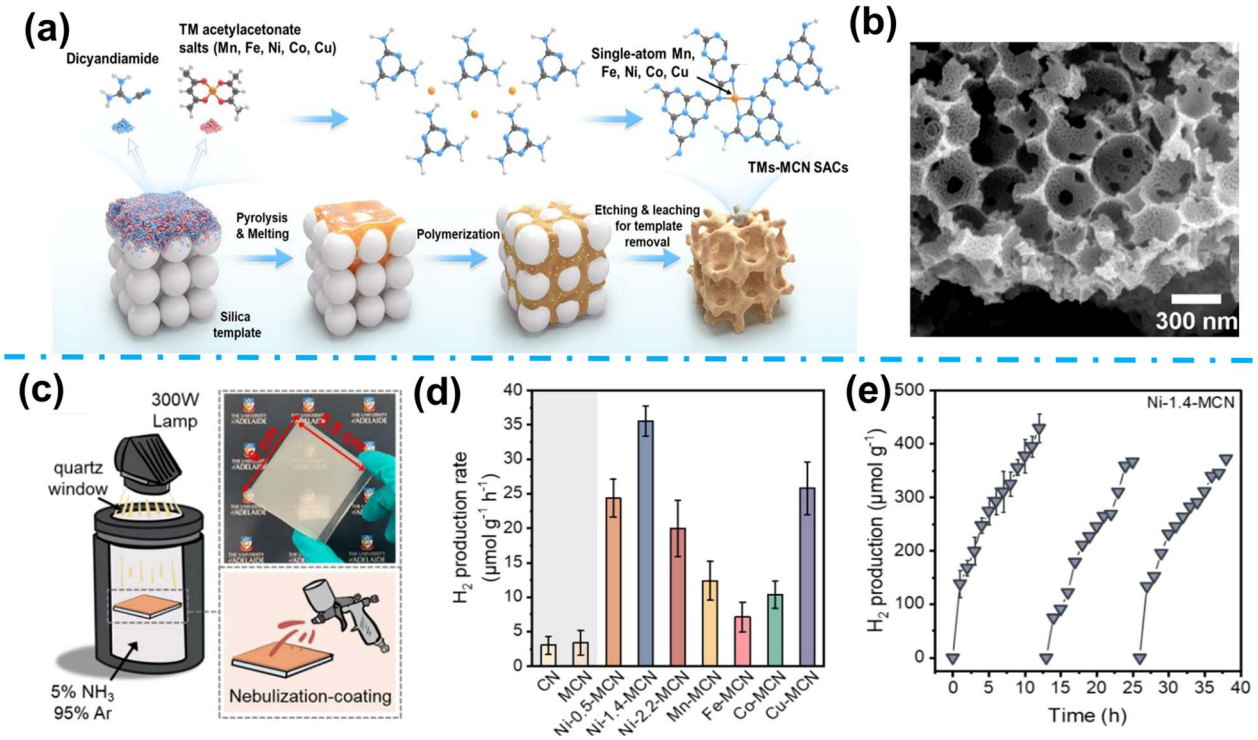

Fig. 3 (a) Schematic illustration of the fabrication process of TMs-MCN SACs. (b) SEM. (c) Schematic illustration of the reaction system and nebulization-coating method. (d) H_2 production rates of CN, MCN, and Ni-MCNs with different Ni loadings and TMs-MCNs and (e) cycling tests.[58] Copyright 2023, American Chemical Society.

a custom-made sealed black PTFE reactor (Fig. 3c). Among them, the optimized Ni-1.4-MCN exhibited a significantly enhanced photocurrent response (Fig. 3d) and achieved a hydrogen production rate of 35.6 μmol g^{-1} h^{-1}, representing a substantial improvement compared to the pristine MCN (Fig. 3e). This enhanced performance was attributed to the electron-rich "nitrogen pot" framework structure, which promotes the formation of M–N_x coordination sites. Specifically, the Ni–N_4 centers improved light absorption, facilitated charge carrier separation and transfer, and accelerated the overall NH_3 splitting kinetics.

4. Photocatalytic ammonia decomposition to hydrogen in the liquid phase

In addition to gas-phase ammonia decomposition, the photocatalytic treatment of ammonia in liquid environments has attracted significant interest. As a hydrogen carrier, ammonia exhibits exceptional solubility in water under ambient conditions, with approximately 700 volumes dissolving in a single volume of water, significantly facilitating its storage and transportation.[59] In addition, ammonia is widely utilized as a feedstock in industrial and agricultural processes, leading to its prevalent presence in industrial effluents and municipal wastewater.[60] Therefore, the catalytic decomposition of ammonia for hydrogen production offers a dual advantage: contributing to sustainable energy generation while simultaneously mitigating environmental pollution. Considering the broad application scenarios, we will separately examine photocatalytic hydrogen production from ammonia solutions of low and high concentrations.

4.1 Low concentration

Ammonia is widely utilized as a fundamental chemical in both industrial and agricultural sectors, and the resulting discharge of ammonia-containing wastewater has emerged as a major source of water pollution. At concentrations exceeding 5 ppm, ammonia can exert pronounced toxic effects on aquatic organisms and pose substantial risks to ecosystem health.[61] According to the World Health Organization (WHO) guidelines, the concentration of ammonia in drinking water should not exceed 1.5 ppm.[62] In order to achieve the removal of ammonia from low concentration ammonia solution, the photocatalytic degradation of ammonia has garnered significant research attention. Efficient photocatalysts will be the key to achieving this reaction. Titanium dioxide (TiO_2), the most representative photocatalyst, has found applications in this field. As early as 2007, commercial TiO_2 exhibited high catalytic activity for ammonia degradation,[63] and subsequent efforts have focused on developing and optimizing TiO_2-based systems for enhanced ammonia decomposition.[64–66] Beyond TiO_2, other photocatalysts such as ZnO,[67] CuO[68] and g-C_3N_4 [69] have also shown promising potential for photocatalytic ammonia treatment. Nevertheless, many existing studies have primarily concentrated on ammonia removal rather than hydrogen production.[70] In 2012, Kominami and co-workers reported that noble metal photodeposition on the surface of commercial P25 enabled the simultaneous degradation of ammonia and production of hydrogen (Fig. 4a). By establishing an oxygen-free environment

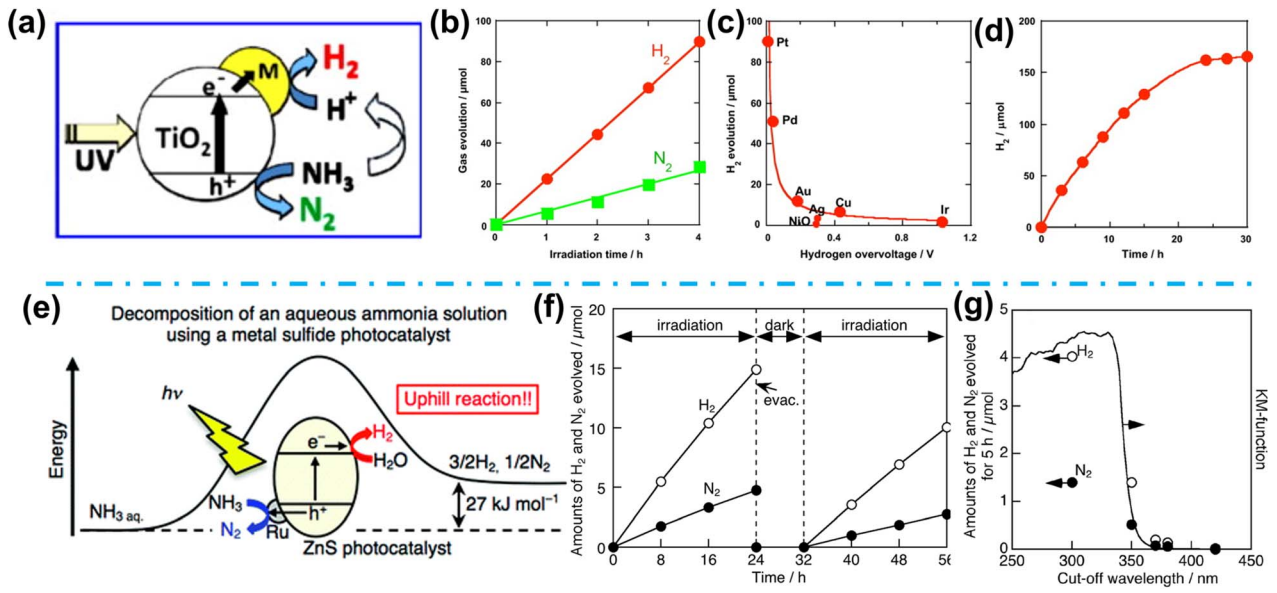

Fig. 4 (a) Schematic diagram of the photocatalytic decomposition of the ammonia based TiO_2 catalyst. (b) Photocatalytic decomposition of ammonia in an aqueous suspension of platinum-loaded TiO_2 particles. (c) Correlation between photocatalytic H_2 evolution and hydrogen overvoltage of metal electrodes. (d) Photocatalytic formation of H_2 from ammonia in an aqueous suspension.[49] Copyright 2012, Elsevier. (e) Schematic diagram of photocatalytic ammonia decomposition. (f) Photocatalytic decomposition of an aqueous ammonia solution over Ru-loaded ZnS under photoirradiation. (g) Wavelength dependencies of the photocatalytic decomposition of an aqueous ammonia solution.[71] Copyright 2017, Elsevier.

to suppress the deep oxidation of ammonia, complete decomposition of ammonia into nitrogen and hydrogen could be achieved (Fig. 4b). The study further demonstrated that the lower the overpotential for the hydrogen evolution reaction (HER), the higher the activity of the co-catalyst for ammonia decomposition. As a result, Pt-loaded TiO_2 showed the highest photocatalytic ammonia decomposition activity (Fig. 4c). Notably, Pt-loaded P25 maintained stable performance for over 20 hours in hydrogen production from ammonia at low concentrations (Fig. 4d).[49]

In addition to platinum, ruthenium (Ru) has also been extensively explored as a co-catalyst for enhancing photocatalytic hydrogen production. Iwase and co-workers successfully loaded Ru onto zinc sulfide (ZnS), one of the most widely studied metal sulfide photocatalysts, and demonstrated its photocatalytic activity for ammonia decomposition in a 20 mmol L^{-1} aqueous solution (Fig. 4e). Under simulated sunlight irradiation, ammonia was decomposed into nitrogen and hydrogen in a stoichiometric ratio. The system was operated continuously for 24 hours, and nitrogen and hydrogen were stably generated (Fig. 4f). Under the irradiation of monochromatic light with a wavelength of 340 nm, the apparent quantum efficiency (AQE) reached 0.21% (Fig. 4g).[71] In addition to loading cocatalysts on the surface of photocatalysts, defect engineering is also an effective method to improve photocatalyst activity.[72,73] Reil synthesized ZnO samples with varying particle sizes, specific surface areas, and defect types by employing different synthetic methods. Even if some samples exhibited higher specific surface areas, excessive defect concentrations led to severe charge carrier trapping, resulting in diminished photocatalytic performance. This finding underscores the crucial role of defects in photocatalysis: a moderate defect concentration can promote charge separation without introducing deep trap states and serve as reaction sites to promote surface reactions, ultimately improving the overall efficiency.[74]

Although photocatalytic technology has demonstrated its photocatalytic activity for ammonia decomposition and hydrogen production at relatively low ammonia concentrations, the overall efficiency remains limited. This limitation primarily arises from the low availability of free ammonia and the dominance of ammonium ions (NH_4^+) under mildly alkaline conditions, which exhibit lower reactivity. To further improve the efficiency and long-term stability of photocatalytic hydrogen production from ammonia, thereby supporting the realization of the Hydrogen 2.0 vision, recent research has increasingly focused on effective strategies for photocatalytic decomposition in higher-concentration ammonia solutions.

4.2 High concentration

Beyond low-concentration wastewater scenarios, the photocatalytic decomposition of ammonia in high-concentration solutions also offers substantial opportunities for hydrogen production. In this review, ammonia solutions with nitrogen concentrations exceeding 1000 ppm are classified as high-concentration ammonia solutions, consistent with typical ammonia levels found in industrial and agricultural wastewater.

Nishiyama and his colleagues synthesized Fe-doped TiO_2 and modulated its bandgap structure without altering its

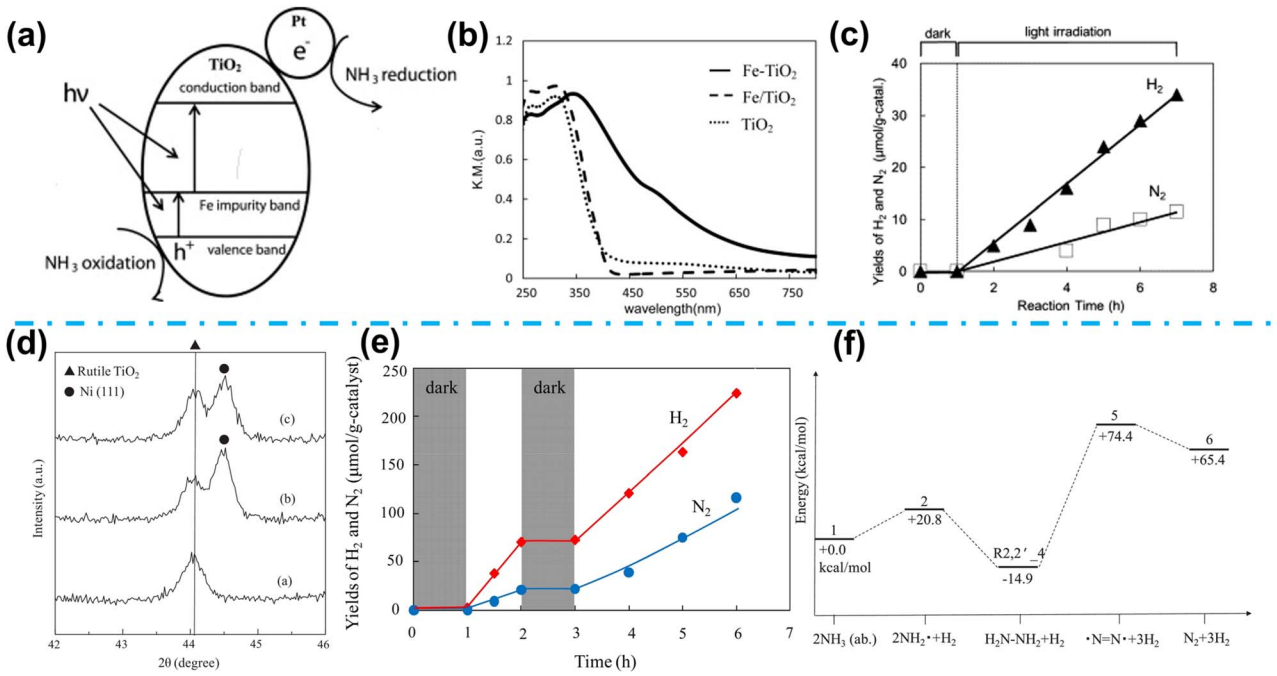

Fig. 5 (a) Schematic diagram of photocatalytic decomposition of ammonia-based Pt/Fe–TiO_2. (b) UV-vis-DR spectra. (c) Time profiles of H_2 and N_2 yields for the photodecomposition of NH_3 solution over Pt/Fe–TiO_2.[75] Copyright 2014, Elsevier. (d) XRD patterns. (e) Time profiles of H_2 and N_2 yields for the NH_3 photodecomposition over Ni/TiO_2. (f) Energy diagram for the NH_3 decomposition to N_2 and H_2.[48] Copyright 2017, Elsevier.

crystalline structure (Fig. 5a). As a result, Fe-doped TiO_2 substituted a portion of the Ti^{4+} sites in TiO_2 and exhibited significantly enhanced visible-light absorption compared to both pristine TiO_2 and photo-deposited iron-modified TiO_2 (Fig. 5b). Upon loading platinum (Pt) as a co-catalyst, the resulting Pt–Fe/TiO_2 exhibited outstanding hydrogen evolution activity (27 μmol g^{-1}) in high-concentration ammonia solutions (Fig. 5c).[75] Notably, no hydrogen production was detected in the absence of ammonia or under dark conditions, confirming that hydrogen generation originated from the light-driven decomposition of ammonia. Although noble metal catalysts such as Pt and Ru exhibit excellent photocatalytic activity, their scarcity and high cost limit their large-scale application. Therefore, efforts have been directed toward developing non-noble metal alternatives. Nickel, recognized as the most efficient non-noble metal catalyst for the thermal decomposition of ammonia, has also been developed to enhance photocatalytic ammonia decomposition for hydrogen production. To prepare metallic Ni, nickel was reduced on the surface of TiO_2 using hydrogen (Fig. 5d). The resulting metallic Ni exhibited superior catalytic activity compared to other transition metal counterparts, including Fe, Co, Cu, and Mn, under identical reaction conditions (Fig. 5e). Furthermore, a possible reaction mechanism for photocatalytic ammonia decomposition mediated by Ni/TiO_2 was proposed (Fig. 5f).[48] Their study demonstrated that H_2 and H_2N–NH_2 as intermediates were formed by the coupling of an NH_2 radical and an NH_3 molecule during the photodecomposition of NH_3.

Due to the inherently wide bandgap of TiO_2, its photocatalytic efficiency is restricted by limited visible-light absorption. Consequently, the development of photocatalysts with narrower bandgaps for ammonia decomposition has emerged as an important strategy. Dzíbelová *et al.* exploited the combination of a conductive 2D Fe_2O_3 substrate with the catalytic surface of RuO_2 nanoparticles to test them as a photocatalytical platform suitable to produce hydrogen under visible light irradiation. Two-dimensional structured Fe_2O_3, with its visible-light responsiveness, has demonstrated efficient photocatalytic ammonia decomposition for hydrogen production in 28% aqueous ammonia solution (Fig. 6a and b), maintaining 89% of its catalytic activity after continuous operation for 120 hours (Fig. 6c). This enhanced photocatalytic performance can be attributed to the synergistic effect of the combination of the RuO_2 surface and 2D hematene substrate on the generation of electrons and holes.[76] However, most semiconductor photocatalysts are ineffective in utilizing infrared light to drive photocatalytic reactions, resulting in significant energy losses. Given that temperature is also a critical factor in ammonia decomposition, photothermal catalysis has gained significant attention. Therefore, converting infrared light into heat through photothermal materials to elevate the reactor temperature and enhance light utilization has emerged as a promising strategy. Zhou *et al.* developed a photo-thermal-catalytic architecture by assembling gallium nitride (GaN) nanowires-supported ruthenium nanoparticles on silicon.[77] In this system, silicon acts as an efficient photothermal substrate, GaN nanowires with a one-

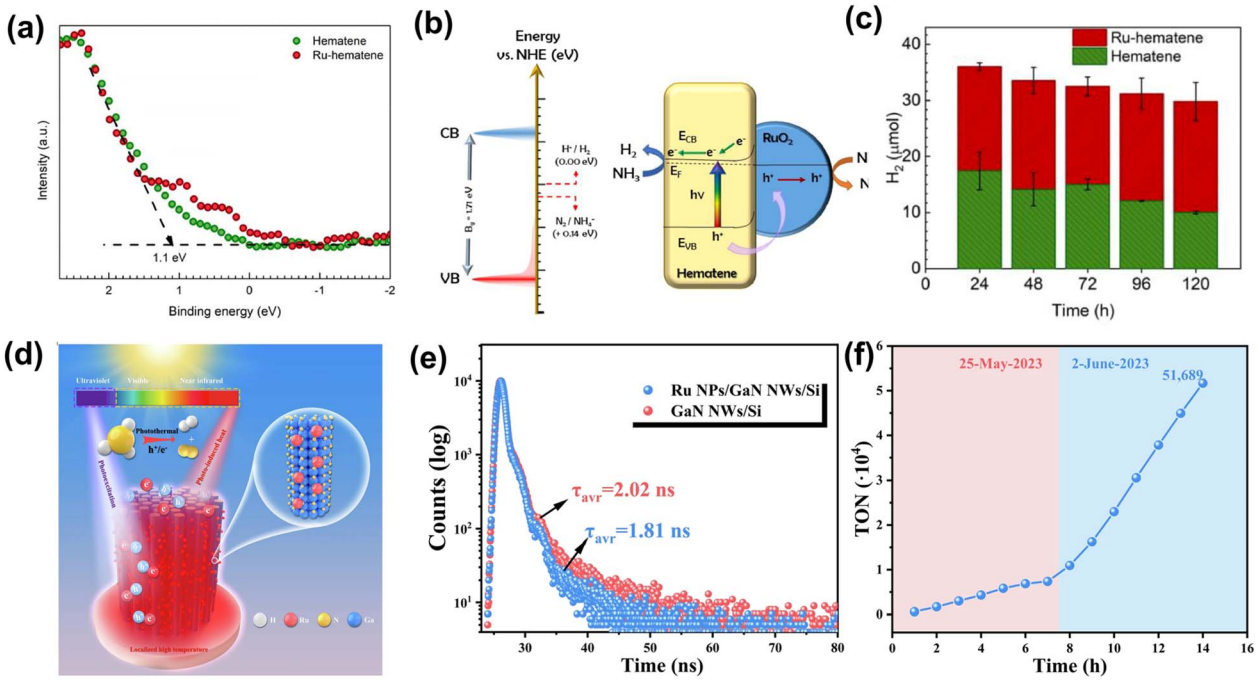

Fig. 6 (a) Valence band XPS of hematene and Ru-hematene. (b) Schematic density of states (DOS) and band edge positions (left) and the proposed mechanism of ammonia photodecomposition by the Ru-hematene photocatalyst. (c) Reusability test for H_2 evolution from ammonia photo decomposition.[76] Copyright 2023, Elsevier. (d) Schematic diagram of the synergy between charge carriers and photo-induced heat for promoting ammonia decomposition. (e) TRPL spectroscopy and (f) TON of Ru NPs/GaN NWs for ammonia decomposition under concentrated natural sunlight without external heating.[77] Copyright 2024, Elsevier.

Table 1 Summary of photocatalytic ammonia decomposition in gas and liquid phases

Catalysts	Ammonia concentration	Light source	HER rate	Stability	Ref.
Cu-Ru-AR	N/-gas	Supercontinuum laser 400–900 nm	1200 μmol g^{-1} s^{-1}	N/A	55
Cu-Fe-AR	N/-gas	LED 400–900 nm	14 g per day	67 h	56
TMs-MCN SACs	N/-gas	Sunlight	35.6 μmol h^{-1}	36 h	58
Pt/TiO_2	0.03 M-liquid	300 W Xe lamp	304 μmol	30 h	49
Ru-loaded ZnS	0.02 M-liquid	UV-25	0.77 μmol h^{-1}	48 h	71
Pt/Fe–TiO_2	0.59 M-liquid	UV-25	33 μmol per g-catal	7 h	75
Ni/TiO_2	0.59 M-liquid	UV-25	131.7 μmol per g-catal	6 h	48
Ru-α-Fe_2O_3	14.6 M-liquid	LED-400–700 nm	28 μmol	120 h	76
Ru NPs/GaN NWs	14.6 M-liquid	AM-1.5G	3.98 mmol cm^{-2} h^{-1}	400 h	77

dimensional structure facilitate charge diffusion and provide abundant active sites for cocatalyst loading, and Ru, owing to its optimal binding strength with reaction intermediates (neither too strong nor too weak), is considered an efficient cocatalyst for photocatalytic ammonia decomposition (Fig. 6d). This design synergistically enhances light absorption, prolongs photogenerated carrier lifetimes, and elevates the reaction temperature, resulting in outstanding photocatalytic performance (Fig. 6e). Moreover, the system demonstrates stable operation under outdoor conditions, highlighting its potential for large-scale, real-world applications (Fig. 6f). Finally, the summary of photocatalytic ammonia decomposition in gas and liquid phases is shown in Table 1.

5. Present challenges and shortcomings

Photocatalytic ammonia degradation holds significant potential for energy sustainability and environmental remediation. Despite recent advances, many challenges remain in both gaseous and aqueous systems, particularly in terms of product selectivity, catalyst stability, and reactor design. A comprehensive understanding of these current limitations is vital for the rational design of efficient, stable and scalable photocatalytic systems for ammonia degradation.

5.1 Selectivity control

Despite the steadily growing interest in photocatalytic ammonia splitting, achieving high product selectivity remains a significant challenge due to undesirable side reactions, especially under oxygen conditions. The presence of oxygen can lead to deeper oxidation, resulting in undesirable byproducts such as NO_x. These byproducts can severely impair the efficiency and selectivity of the reaction.[78,79] Therefore, it is crucial to establish an oxygen-free reaction environment for selective nitrogen and hydrogen generation. Apart from that, developing efficient catalysts is also important to improve selectivity. Suitable catalysts can favour the formation of desired products by adjusting the activation energy of the intermediates. It will interact strongly with ammonia while minimizing side reactions, thereby enhancing selectivity and long-time stability.

5.2 Catalyst durability and surface deactivation

Under long-term light conditions, the catalyst will inevitably degrade and deactivate.[80,81] The occurrence of these phenomena is usually attributed to the irreversible adsorption or accumulation of nitrogen-containing intermediates (such as NO, NO_2^-, and NH_4^+) on the catalyst surface. It will significantly reduce the number of accessible active sites, hinder charge carrier separation, and ultimately affect catalytic efficiency. Besides, the formation of surface passivation layers composed of oxidative byproducts can obstruct light collection and limit the diffusion of reactants, ultimately leading to increased costs. To address these issues, new strategies such as constructing surface passivation and developing regenerative photocatalysts are urgently needed.[82–85] These approaches are expected to enhance the long-term structural stability of catalysts and support the practical application of photocatalytic ammonia conversion technologies.

5.3 Large-scale application of photocatalytic technology

Although significant progress has been made at the laboratory scale, large-scale implementation of photocatalytic ammonia conversion remains challenging. In gas-phase applications, scalable systems must overcome limitations related to light penetration and gas–solid mass transfer, while liquid-phase systems present challenges such as low diffusion rates, catalyst recovery and operational stability in dynamic aqueous environments. Furthermore, successful translation from laboratory to real applications will critically depend on techno-economic feasibility, environmental sustainability and so on. From a long-term perspective, the rational development of photocatalytic platforms should also consider practical feasibility and environmental compatibility. Solving these problems will promote the further development of practical applications of photocatalytic systems for NH_3 emission reduction and sustainable nitrogen cycle remediation.

6. Summary and perspectives

This review provides a comprehensive overview of recent advances in photocatalytic ammonia decomposition for hydrogen production. First, the basic principles of photocatalysis are introduced. Photocatalytic technology is widely applied in both environmental remediation and energy

conversion, and well-suited to meet the requirements of ammonia to hydrogen conversion. The possible reaction mechanisms of photocatalytic ammonia decomposition are discussed. Considering the differences between gas and liquid phase systems, the current state of research under both conditions is reviewed, respectively. Strategies such as catalyst optimization and reaction system design have been explored to improve hydrogen production efficiency. Finally, the existing challenges and limitations in this field are briefly outlined. Due to the limited number of relevant studies, further research is needed to promote the progress and development of this field.

In recent years, with the continuous progress of photocatalysis research, various strategies have been developed to enhance photocatalyst performance, including the construction of heterojunctions, single-atom catalyst engineering and defects engineering.[86–88] Such methods have been widely applied in various photocatalytic processes, including hydrogen evolution, carbon dioxide reduction and organic pollutant degradation.[89,90] Some of these strategies have also been used to develop more active ammonia splitting photocatalysts. However, the development and application of these advanced techniques in this specific field are still incomplete and require further research.

Ammonia decomposition is an uphill reaction that requires a large amount of energy input, so temperature is a critical factor influencing the overall reaction efficiency.[91] In photocatalytic processes, most photocatalysts are limited to absorbing ultraviolet and a small part of visible light, resulting in most of the solar energy not being fully utilized.[92,93] In the past few years, increasing attention has been directed toward photothermal-assisted catalysis as a promising strategy for efficient ammonia decomposition.[94] By rationally designing catalyst structures capable of absorbing infrared light, the local reaction temperature can be increased, and catalyst aggregation can be suppressed. Another promising approach is photoelectrocatalysis, which has achieved remarkable success in addressing key challenges in photocatalytic processes, such as poor product selectivity and low charge carrier separation efficiency.[95–97] These advancements are expected to provide new directions for achieving efficient photocatalytic ammonia decomposition and accelerating progress in this field.

With the continuous advancement in catalyst development and a deeper understanding of photocatalytic reaction mechanisms, the efficiency of photocatalytic ammonia decomposition has gradually improved.[98] Accordingly, the large-scale application of this technology for hydrogen production is undoubtedly the goal. In recent years, increasing attention has been devoted to the scale-up of photocatalytic technologies. Encouragingly, in the field of photocatalytic water splitting, continuous and stable hydrogen production has already been demonstrated at the 100 m^2 scale, proving the feasibility of scaling up photocatalysis.[99] For photocatalytic ammonia decomposition, which is inherently a more complex reaction, existing studies have successfully achieved light harvesting and hydrogen production under natural sunlight, pointing the way forward for future progress toward large-scale application in this field.

In summary, despite significant progress in the field of photocatalytic ammonia decomposition for hydrogen production, many challenges remain. Based on current research, the design of photocatalysts should be further optimized to face existing problems. In addition, developing scalable reactor technologies is crucial for establishing more efficient, stable, and large-scale systems for photocatalytic ammonia decomposition to produce hydrogen. Ultimately, it provides a strategic solution for mitigating ammonia-related environmental pollution and promoting carbon-free hydrogen energy development.

Author contributions

Qian Lei and Huazhang Feng conducted the data curation, investigation, manuscript writing, review and editing parts of the paper. Yuankai Li assisted with data curation and investigation. Jung Kyu Kim contributed to the funding acquisition, conceptualisation, project administration and supervision of the topic, as well as the manuscript writing and review.

Conflicts of interest

There are no conflicts to declare.

Data availability

No primary research results, software or code have been included, and no new data were generated or analysed as part of this review.

Acknowledgements

This work was supported by the National Research Foundation of Korea (NRF) grant funded by the Korea government (MSIT) (No. RS-2024-00467234) and Korea Institute of Science and Technology (KIST) Institutional Program (2E33251).

References

1 M. Farghali, A. I. Osman, I. M. Mohamed, Z. Chen, L. Chen, I. Ihara, P. S. Yap and D. W. Rooney, *Environ. Chem. Lett.*, 2023, **21**, 2003–2039.
2 C. Xia, S. Surendran, S. Ji, D. Kim, Y. Chae, J. Kim, M. Je, M. K. Han, W. S. Choe and C. H. Choi, *Carbon Energy*, 2022, **4**, 491–505.
3 A. Rahman, O. Farrok and M. M. Haque, *Renewable Sustainable Energy Rev.*, 2022, **161**, 112279.
4 X. L. Yang, Y. W. Lv, J. Hu, J.-R. Zhao, G. Y. Xu, X. Q. Hao, P. Chen and M.-Q. Yan, *RSC Adv.*, 2021, **11**, 17352–17359.
5 M. Asif, S. S. Bibi, S. Ahmed, M. Irshad, M. S. Hussain, H. Zeb, M. K. Khan and J. Kim, *Chem. Eng. J.*, 2023, **473**, 145381.
6 C. Pei, M. C. Kim, Y. Li, C. Xia, J. Kim, W. So, X. Yu, H. S. Park and J. K. Kim, *Adv. Funct. Mater.*, 2023, **33**, 2210072.
7 Y. Li, M. C. Kim, C. Xia, W. T. Hong, J. Kim, G. Bae, Y. S. Jang, S. Y. Jeong, E. Sim and C. H. Choi, *Appl. Catal., B*, 2024, **343**, 123516.

8 S. O. Bade, O. S. Tomomewo, A. Meenakshisundaram, P. Ferron and B. A. Oni, *Int. J. Hydrogen Energy*, 2024, **49**, 314–335.
9 X. Xi, Y. Fan, K. Zhang, Y. Liu, F. Nie, H. Guan and J. Wu, *Chem. Eng. J.*, 2022, **435**, 134818.
10 S. Yin, B. Xu, X. Zhou and C. Au, *Appl. Catal., A*, 2004, **277**, 1–9.
11 Y. Kojima and M. Yamaguchi, *Int. J. Hydrogen Energy*, 2022, **47**, 22832–22839.
12 S. Sun, Q. Jiang, D. Zhao, T. Cao, H. Sha, C. Zhang, H. Song and Z. Da, *Renewable Sustainable Energy Rev.*, 2022, **169**, 112918.
13 A. T. Wijayanta, T. Oda, C. W. Purnomo, T. Kashiwagi and M. Aziz, *Int. J. Hydrogen Energy*, 2019, **44**, 15026–15044.
14 N. Bora, A. K. Singh, P. Pal, U. K. Sahoo, D. Seth, D. Rathore, S. Bhadra, S. Sevda, V. Venkatramanan and S. Prasad, *Fuel*, 2024, **369**, 131808.
15 L. Babcock-Jackson, T. Konovalova, J. P. Krogman, R. Bird and L. L. Díaz, *J. Agric. Food Chem.*, 2023, **71**, 8265–8296.
16 K. Adeli, M. Nachtane, A. Faik, D. Saifaoui and A. Boulezhar, *Appl. Sci.*, 2023, **13**, 8711.
17 K. Vikrant, K. H. Kim, F. Dong and D. A. Giannakoudakis, *ACS Catal.*, 2020, **10**, 8683–8716.
18 P. R. Lakshmi, B. Mohan, P. Kang, P. Nanjan and S. Shanmugaraju, *Chem. Commun.*, 2023, **59**, 1728–1743.
19 D. W. Kang, S. E. Ju, D. W. Kim, M. Kang, H. Kim and C. S. Hong, *Adv. Sci.*, 2020, **7**, 2002142.
20 S. Zhang, D. Li, S. Ge, S. Liu, C. Wu, Y. Wang, Y. Chen, S. Lv, F. Wang and J. Meng, *Sci. Total Environ.*, 2021, **772**, 144897.
21 M. Li, C. J. Weschler, G. Beko, P. Wargocki, G. Lucic and J. Williams, *Environ. Sci. Technol.*, 2020, **54**, 5419–5428.
22 K. Guo, J. Ji, W. Song, J. Sun, C. Tang and L. Dong, *Appl. Catal., B*, 2021, **297**, 120388.
23 S. Sarkar, S. S. Gill, G. Das Gupta and S. Kumar Verma, *Environ. Sci. Pollut. Res.*, 2022, **29**, 53934–53953.
24 R. Nieder and D. K. Benbi, *Rev. Environ. Health*, 2022, **37**, 229–246.
25 Y. Hu and U. Schmidhalter, *Environ. Sustain. Indic.*, 2024, **22**, 100365.
26 S. Peters, A. M. Abdel Mageed and S. Wohlrab, *ChemCatChem*, 2023, **15**, e202201185.
27 T. A. Le, Q. C. Do, Y. Kim, T.-W. Kim and H.-J. Chae, *Korean J. Chem. Eng.*, 2021, **38**, 1087–1103.
28 C. Chen, K. Wu, H. Ren, C. Zhou, Y. Luo, L. Lin, C. Au and L. Jiang, *Energy Fuels*, 2021, **35**, 11693–11706.
29 A. Kumar, V. Vibhu, J. M. Bassat, L. Nohl, L. de Haart, M. Bouvet and R. A. Eichel, *ChemElectroChem*, 2024, **11**, e202300845.
30 L. Luo, T. Zhang, M. Wang, R. Yun and X. Xiang, *ChemSusChem*, 2020, **13**, 5173–5184.
31 H. Duan, F. Kong, X. Bi, L. Chen, H. Chen, D. Yang and W. Huang, *ACS Catal.*, 2024, **14**, 17972–17992.
32 Y. Shu, D. Wang, J. Wang and H. Huang, *Chem. Eng. J.*, 2024, 154925.
33 F. Chang, W. Gao, J. Guo and P. Chen, *Adv. Mater.*, 2021, **33**, 2005721.
34 Y. Zhang, Y. Ji, J. Li, J. Bai, S. Chen, L. Li, J. Wang, T. Zhou, P. Jiang and X. Guan, *J. Hazard. Mater.*, 2021, **402**, 123725.
35 H. Pan, J. Li, Y. Wang, Q. Xia, L. Qiu and B. Zhou, *Adv. Sci.*, 2024, **11**, 2402651.
36 X. Li, Y. Chen, Y. Tao, L. Shen, Z. Xu, Z. Bian and H. Li, *Chem Catal.*, 2022, **2**, 1315–1345.
37 M. Xiao, Z. Wang, M. Lyu, B. Luo, S. Wang, G. Liu, H. M. Cheng and L. Wang, *Adv. Mater.*, 2019, **31**, 1801369.
38 L. Zhang, J. Zhang, H. Yu and J. Yu, *Adv. Mater.*, 2022, **34**, 2107668.
39 W. Jiang, H. Loh, B. Q. L. Low, H. Zhu, J. Low, J. Z. X. Heng, K. Y. Tang, Z. Li, X. J. Loh and E. Ye, *Appl. Catal., B*, 2023, **321**, 122079.
40 S. Bai, N. Zhang, C. Gao and Y. Xiong, *Nano Energy*, 2018, **53**, 296–336.
41 C. Sun, J. Yang, M. Xu, Y. Cui, W. Ren, J. Zhang, H. Zhao and B. Liang, *Chem. Eng. J.*, 2022, **427**, 131564.
42 F. Gao, Y. Zhao, X. Zhang and J. You, *Adv. Energy Mater.*, 2020, **10**, 1902650.
43 Q. Su, Y. Li, R. Hu, F. Song, S. Liu, C. Guo, S. Zhu, W. Liu and J. Pan, *Adv. Sustainable Syst.*, 2020, **4**, 2000130.
44 G. Zhang, Z. Wang and J. Wu, *Nanoscale*, 2021, **13**, 4359–4389.
45 C. Liu, S. Mao, M. Shi, X. Hong, D. Wang, F. Wang, M. Xia and Q. Chen, *Chem. Eng. J.*, 2022, **449**, 137757.
46 Y. He, Q. Lei, C. Li, Y. Han, Z. Shi and S. Feng, *Mater. Today*, 2021, **50**, 358–384.
47 H. Zhao, Q. Mao, L. Jian, Y. Dong and Y. Zhu, *Chin. J. Catal.*, 2022, **43**, 1774–1804.
48 A. Utsunomiya, A. Okemoto, Y. Nishino, K. Kitagawa, H. Kobayashi, K. Taniya, Y. Ichihashi and S. Nishiyama, *Appl. Catal., B*, 2017, **206**, 378–383.
49 H. Yuzawa, T. Mori, H. Itoh and H. Yoshida, *J. Phys. Chem. C*, 2012, **116**, 4126–4136.
50 Q. Pei, Y. Wang, K. C. Tan, J. Guo, T. He and P. Chen, *Chem. Sci.*, 2025, **16**, 9076–9091.
51 R. Asahi, T. Morikawa, H. Irie and T. Ohwaki, *Chem. Rev.*, 2014, **114**, 9824–9852.
52 G. Liu, H. G. Yang, J. Pan, Y. Q. Yang, G. Q. Lu and H.-M. Cheng, *Chem. Rev.*, 2014, **114**, 9559–9612.
53 Y. Zhang, S. He, W. Guo, Y. Hu, J. Huang, J. R. Mulcahy and W. D. Wei, *Chem. Rev.*, 2017, **118**, 2927–2954.
54 B. Y. Zheng, H. Zhao, A. Manjavacas, M. McClain, P. Nordlander and N. J. Halas, *Nat. Commun.*, 2015, **6**, 7797.
55 L. Zhou, D. F. Swearer, C. Zhang, H. Robatjazi, H. Zhao, L. Henderson, L. Dong, P. Christopher, E. A. Carter and P. Nordlander, *Science*, 2018, **362**, 69–72.
56 Y. Yuan, L. Zhou, H. Robatjazi, J. L. Bao, J. Zhou, A. Bayles, L. Yuan, M. Lou, M. Lou, S. Khatiwada, E. A. Carter, P. Nordlander and H. J. Halas, *Science*, 2022, **378**, 889–893.
57 H. Zhang, W. Tian, X. Duan, H. Sun, S. Liu and S. Wang, *Adv. Mater.*, 2020, **32**, 1904037.
58 J. Lin, Y. Wang, W. Tian, H. Zhang, H. Sun and S. Wang, *ACS Catal.*, 2023, **13**, 11711–11722.
59 M. El-Bourawi, M. Khayet, R. Ma, Z. Ding, Z. Li and X. Zhang, *J. Membr. Sci.*, 2007, **301**, 200–209.

60 M. Sheikh, H. R. Harami, M. Rezakazemi, J. L. Cortina, T. M. Aminabhavi and C. Valderrama, *Sci. Total Environ.*, 2023, **904**, 166077.
61 N. Liu, Z. Sun, H. Zhang, L. H. Klausen, R. Moonhee and S. Kang, *Sci. Total Environ.*, 2023, **875**, 162603.
62 Y.-J. Shih and C.-H. Hsu, *Chem. Eng. J.*, 2021, **409**, 128024.
63 S. Yamazoe, T. Okumura and T. Tanaka, *Catal. Today*, 2007, **120**, 220–225.
64 F. Dalanta and T. D. Kusworo, *Chem. Eng. J.*, 2022, **434**, 134687.
65 F. Yao, W. Fu, X. Ge, L. Wang, J. Wang and W. Zhong, *Sci. Total Environ.*, 2020, **727**, 138425.
66 Q. Zhou, H. Yin, A. Wang and Y. Si, *Chin. J. Chem. Eng.*, 2019, **27**, 2535–2543.
67 N. Tafreshi, S. Sharifnia and S. M. Dehaghi, *Process Saf. Environ.*, 2017, **106**, 203–210.
68 Y. Shavisi, S. Sharifnia and Z. Mohamadi, *J. Environ. Chem. Eng.*, 2016, **4**, 2736–2744.
69 H. Wang, Y. Su, H. Zhao, H. Yu, S. Chen, Y. Zhang and X. Quan, *Environ. Sci. Technol.*, 2014, **48**, 11984–11990.
70 H. Kominami, H. Nishimune, Y. Ohta, Y. Arakawa and T. Inaba, *Appl. Catal., B*, 2012, **111**, 297–302.
71 A. Iwase, K. Ii and A. Kudo, *Chem. Commun.*, 2018, **54**, 6117–6119.
72 J.-Y. Qiu, H. Z. Feng, Z. H. Chen, S. H. Ruan, Y. P. Chen, T. T. Xu, J. Y. Su, E. N. Ha and L. Y. Wang, *Rare Met.*, 2022, **41**, 2074–2083.
73 H. Feng, Z. Chen, C. Lin, Y. Chen, J. Su, E. Ha, K. Zhang and L. Wang, *Int. J. Hydrogen Energy*, 2024, **96**, 255–263.
74 M. Reli, M. Edelmannová, M. Šihor, P. Praus, L. Svoboda, K. K. Mamulová, H. Otoupalíková, L. Čapek, A. Hospodková and L. Obalová, *Int. J. Hydrogen Energy*, 2015, **40**, 8530–8538.
75 K. Obata, K. Kishishita, A. Okemoto, K. Taniya, Y. Ichihashi and S. Nishiyama, *Appl. Catal., B*, 2014, **160**, 200–203.
76 J. Dzíbelová, S. H. Hejazi, V. Šedajová, D. Panáček, P. Jakubec, Z. Baďura, O. Malina, J. Kašlík, J. Filip and Š. Kment, *Appl. Mater. Today*, 2023, **34**, 101881.
77 J. Li, B. Sheng, Y. Chen, J. Yang, P. Wang, Y. Li, T. Yu, H. Pan, L. Qiu, Y. Li, J. Song, L. Zhu, X. Wang, Z. Huang and B. Zhou, *Nat. Commun.*, 2024, **15**, 7393.
78 Z. ur Rahman, X. Wang, H. Mikulcic, S. Zhou, J. Zhang, M. Vujanovic and H. Tan, *J. Energy Inst.*, 2022, **100**, 89–98.
79 T. K. C. Phu, W. T. Hong, H. Han, Y. I. Song, J. H. Kim, S. H. Roh, M.-C. Kim, J. H. Koh, B.-K. Oh and J. Y. Kim, *Mater. Today*, 2024, **76**, 52–63.
80 C. H. Bartholomew, *Appl. Catal., A*, 2001, **212**, 17–60.
81 A. J. Martín, S. Mitchell, C. Mondelli, S. Jaydev and J. Pérez-Ramírez, *Nat. Catal.*, 2022, **5**, 854–866.
82 Y. Zhang, X. Wu, Z. H. Wang, Y. Peng, Y. Liu, S. Yang, C. Sun, X. Xu, X. Zhang and J. Kang, *J. Am. Chem. Soc.*, 2024, **146**, 6618–6627.
83 Y. Wan, J. Li, J. Ni, C. Wang, C. Ni and H. Chen, *J. Hazard. Mater.*, 2022, **435**, 129073.
84 D. Ma, J. Chen, J. Li, X. Ji and J. W. Shi, *J. Mater. Chem. A*, 2024, **12**, 12293–12324.
85 C. Xia, Y. Li, M. Je, J. Kim, S. M. Cho, C. H. Choi, H. Choi, T.-H. Kim and J. K. Kim, *Nano–Micro Lett.*, 2022, **14**, 209.
86 Z.-H. Xue, D. Luan, H. Zhang and X. W. D. Lou, *Joule*, 2022, **6**, 92–133.
87 H. Zhang, W. Cheng, D. Luan and X. W. Lou, *Angew. Chem., Int. Ed.*, 2021, **60**, 13177–13196.
88 Z. Wang, X. Yuan, H. Guo, X. Zhang, J. Peng and Y. Pan, *Energy Environ. Sci.*, 2024, **17**, 8019–8056.
89 J. An, S. Ge, G. Wang and H. Fu, *Energy Environ. Sci.*, 2024, **17**, 5039–5047.
90 Y. Li, J. Kim, W. T. Hong, J. Y. Kim, Q. Lei, H. Han, U. Baeck, D. H. Kim, C. H. Choi and B. H. Kim, *ACS Energy Lett.*, 2025, **10**, 2305–2314.
91 S. Zhang, Z. He, X. Li, J. Zhang, Q. Zang and S. Wang, *Nanoscale Adv.*, 2020, **2**, 3610–3623.
92 G. Han, G. Li, J. Huang, C. Han, C. Turro and Y. Sun, *Nat. Commun.*, 2022, **13**, 2288.
93 A. Wang, S. Wu, J. Dong, R. Wang, J. Wang, J. Zhang, S. Zhong and S. Bai, *Chem. Eng. J.*, 2021, **404**, 127145.
94 Y. Zhou, Y. Feng, H. Xie, J. Lu, D. Ding and S. Rong, *Appl. Catal., B*, 2023, **331**, 122668.
95 C. Xia, Y. Li, H. Kim, K. Kim, W. S. Choe, J. K. Kim and J. H. Park, *J. Hazard. Mater.*, 2021, **408**, 124900.
96 Y. M. Choi, B. W. Lee, M. S. Jung, H. S. Han, S. H. Kim, K. Chen, D. H. Kim, T. F. Heinz, S. Fan and J. Lee, *Adv. Energy Mater.*, 2020, **10**, 2000570.
97 S. H. Roh, E. Kwak, W. T. Hong, C. Xia, S. Kim, H. Chae, X. Yu, W. Yang, J. Park and J. K. Kim, *SusMat*, 2025, **5**, e253.
98 L. Lin, Y. Ma, J. J. M. Vequizo, M. Nakabayashi, C. Gu, X. Tao, H. Yoshida, Y. Pihosh, Y. Nishina and A. Yamakata, *Nat. Commun.*, 2024, **15**, 397.
99 H. Nishiyama, T. Yamada, M. Nakabayashi, Y. Maehara, M. Yamaguchi, Y. Kuromiya, Y. Nagatsuma, H. Tokudome, S. Akiyama and T. Watanabe, *Nature*, 2021, **598**, 304–307.